AN INVESTIGATION OF SWEPTBACK WING ROOT STRESSES

A THESIS

Presented to

the Faculty of the Graduate Division

by

William Myron Eason

In Partial Fulfillment

of the Requirements for the Degree

Master of Science

in the School of Aeronautical Engineering

Georgia Institute of Technology

June, 1955

In presenting the dissertation as a partial fulfillment of the requirements for an advanced degree from the Georgia Institute of Technology, I agree that the Library of the Institution shall make it available for inspection and circulation in accordance with its regulations governing materials of this type. I agree that permission to copy from, or to publish from, this dissertation may be granted by the professor under whose direction it was written, or, in his absence, by the Dean of the Graduate Division when such copying or publication is solely for scholarly purposes and does not involve potential financial gain. It is understood that any copying from, or publication of, this dissertation which involves potential financial gain will not be allowed without written permission.

_____

AN INVESTIGATION OF SWEPTBACK

WING ROOT STRESSES

Approved:

Date Approved by Chairman May 14, 1955

ACKNOWLEDGEMENTS

On the completion of this work I wish to express my sincerest appreciation to Professor G. K. Williams for his most valuable guidance and aid in its prosecution. I should also like to thank Professor J. J. Harper and Professor R. K. Jacobs who were kind enough to serve on the reading committee.

TABLE OF CONTENTS

LIST OF TABLES

LIST OF FIGURES

Figure Page

LIST OF SYMBOLS

U_i	Total internal strain energy
U_e	Total potential energy of the external loads
ℓ	Length of outer wing section
ℓ_1	Half the height of the rear spar
ℓ_2	Half the rib length
ℓ_3	Half the height of the front spar
A_1, A_4	Cross-sectional area of the spar flanges
b	Width of cross section of the box beam measured perpendicularly to the spars
h	Depth of cross section of the box beam
t_c	Thickness of the cover skin
t_w	Thickness of the spar webs
t_1	Thickness of the rear spar web
t_2	Thickness of the cover skin
t_3	Thickness of the front spar web
t_s	Thickness of sheet equivalent to the stringers
k_1	$A_1/2t_2\ell_2$
k_3	$A_3/2t_2\ell_2$
K	$\frac{\sin^2}{E'} + \frac{\cos^2}{G}$
x	Span station measured outboard along the outer wing section
E	Modulus of elasticity of the material

G	Modulus of rigidity of the material
E'	$E/(1-\mu^2)$
R_1	Reactions in the spar flanges at the juncture of the inner and outer sections of the sweptback box beam
P	Shear load applied at the wing tip
a_o, b_o	Constants used in solving for the coefficients C
α	Sweepback angle
ϕ	Angle between the tangent to the rib in the plane of the rib and a line parallel to the center line of the beam
T	Constant torque load applied in the plane of the rib at the wing tip
M_y	Moment about the y axis applied at the tip of the box beam
β	Constant defined by Eq. (12)
τ_c	Shear stresses in the cover skin
τ_w	Shear stresses in the spar webs
σ_1, σ_4	Normal stresses in the spar flanges
f_2	Direct stress parallel to the stringers in the cover due to the bending moment in the cover taken by the skin

SUMMARY

An investigation was made of the methods which have been proposed for the calculations of sweptback wing stresses, and a brief description of each method given in the introduction of this thesis.

The shear stresses in the webs and the normal stresses in the flanges of a sweptback box beam which was tested by the National Advisory Committee for Aeronautics at Langley Field, Virginia, with a concentrated load applied at the tip were calculated by using a simplified method of minimum potential energy. These theoretical values were plotted against the stresses obtained experimentally for this beam and a comparison was made of the results. They were then cross-plotted against the theoretical and experimental values obtained in a test of a similar sweptback box beam at Massachusetts Institute of Technology, and a further comparison made.

The theoretical shear stresses in the webs and covers of the sweptback box beam tested by the National Advisory Committee for Aeronautics when loaded by a constant torque load applied at the tips were calculated by two different methods. One was the simplified method of minimum potential energy, and the other was a method developed by Mr. J. J. Thompson and Mr. W. H. Wittrick of the University of Sydney, Australia. The theoretical and experimental values of these stresses were then compared.

CHAPTER I

INTRODUCTION

The calculation of the stress distribution in the vicinity of the root of a sweptback box beam is a very difficult problem. Several methods have been proposed for the calculations of these stresses, but most of these methods are very cumbersome to use. What is needed is a method of solution that is not too difficult for use in preliminary design calculations but which will still give reasonably good results for the stress distribution, especially in the vicinity of the root.

It has been found by experiment that the stresses in a sweptback box beam at a section remote from the root can be predicted very accurately by the elementary methods for an unswept box beam. Furthermore, experiments indicate that there is a relief of stresses in the vicinity of the front spar at the root and an increase of the stresses in the vicinity of the rear spar at the root that cannot be predicted by the simple methods.

Up until the present time there has been very little material published on the subject of the calculations of sweptback box beam stresses. A method has been described by Levy (1) by which the stresses and deflections in sweptback box beams with ribs parallel to the airstream can be computed. In this method the wing is broken down into structural units. The number of unknown internal forces depends on the number of structural units which make up the wing. Then the equations

of equilibrium are written for these structural units. In those cases where equilibrium conditions are not sufficient in themselves to determine the stress distribution, additional equations may be written by considering the fact that the actual distribution corresponds to a minimum of the strain energy. This condition, called the principle of minimum complementary energy, is a variational condition on the stresses. It is a condition which defines the correct state of stress, among all possible states of stress, that satisfies the conditions of equilibrium. Enough equations may be written utilizing the principle of minimum complementary energy so that the total number of equations is equal to the total number of unknowns. These equations are then solved simultaneously by matrix methods.

Bisplinghoff and Lang (2) have developed a modified Levy method by which a sweptback box beam having the ribs perpendicular to the spars can be analyzed. It has been observed by experiment that, at a distance sufficiently removed from the root, the stresses in a sweptback wing of fairly high aspect ratio may be predicted accurately by the ordinary unswept box beam theories. In the modified Levy method the outboard portion of the wing is analyzed using the ordinary St. Venant theory of bending and torsion in which the cross-sections are assumed free to warp. In the inboard portion, the same procedures suggested by Levy are used to introduce the restraining influence of the root. The strain energies in the inner and outer sections are added, finally, to determine the matrix of influence coefficients.

Bisplinghoff and Lang (3) also describe a method of minimum potential energy in which the assumption is made that the root rib is

elastic and all the other ribs are rigid. The method is very similar to the Levy method in that the structure is broken down into its structural units and equilibrium equations are written for these members. The additional equations in the minimum potential energy method are written, utilizing a variational condition on the displacements, however, instead of a variational condition on the stresses, as in the Levy method. The variational condition on the displacements determines the deformation configuration, among all possible deformations consistent with the boundary conditions, that satisfies equilibrium. These equations are then solved by matrix methods in the same manner as those of the Levy method.

Zender, Heldenfels, and Libove (4) present a method for the analysis of a 45° sweptback box beam having ribs perpendicular to the spars and having an elastic carry-through structure. The carry-through structure is a section of rectangular box beam which connects the sweptback portions of the box beam and simulates the fuselage structure to which the sweptback beams would be attached on an airplane. In this method the outer sections and carry-through bay are analyzed by the simple methods used for unswept box beams. Then the triangular section joining them is divided into free bodies and equilibrium and continuity equations are written. A system of linear equations results which can be solved for the rotations and translations of the vertical edges of the triangular section. Since the unknown internal forces in the structural members and the joint displacements are both related to the applied loads, force-displacement relationships may be written, utilizing certain stiffness parameters which include both the shear and bending

resistance of the beam, to define relationships between the joint displacements and the internal forces. By using these relationships the forces in the equilibrium equations can be replaced by the loads applied to the structure and the joint displacements. These equations can then be solved simultaneously, by matrix methods, for the displacements. Once the joint displacements are known the stresses and distortions of the entire structure may be determined by using the force-displacement relationships again.

Wittrick and Thompson (5,6) have developed a method based on the work of Hadji-Argyris (7) for calculating the stress distribution in a swept tube with ribs parallel to the airstream. In this derivation the assumption is made that the section of the tube is maintained by closely spaced ribs which are rigid in their own planes and unable to offer any resistance to warping out of their planes. The method was derived for the loading conditions of a constant bending moment applied at the tip, a constant torque applied at the tip, and for an exponentially varying load. It was also derived for a tube of arbitrary cross-section. In this method the structure is broken up into its components and equilibrium and continuity equations are written. The elementary expressions for stresses, strains, displacements, and rotations are used, and, except for the differences in geometry, the analysis is very similar to one for an unswept tube or box beam. It is shown later on that for the case of ribs perpendicular to the spars this method reduces to the elementary formulas for stresses in an unswept box beam. This method does not take into account the variation of stresses in the vicinity of the root.

The simplified minimum potential energy method developed by Bisplinghoff and Lang (8) is, as the name implies, a simplified method utilizing the principle of minimum potential energy. The principle of minimum potential energy is, as defined earlier, a variational condition on the displacements which determines the deformation configuration, among all possible deformations consistent with the boundary conditions, that satisfies equilibrium. In the simplified method of minimum potential energy the principle of minimum potential energy is applied to the outboard section of a sweptback box beam as if it were an unswept box beam attached to an elastic support. A simplified analysis, also utilizing the principle of minimum potential energy, is made of the triangular inboard section to determine the properties of the elastic support. An equation of continuity is then written which requires that the warping across the section at the juncture of the inboard and outboard sections be equal in each. The assumption is made in this analysis that a large number of closely spaced ribs, completely rigid in their own planes, are used to preserve the cross section of the wing at all points along the span. The problem is simplified considerably by this assumption, and the errors which are introduced are of second order importance.

The methods described herein comprise the main published theoretical literature on the sweptback beam problem.

The purpose of this thesis is to compare theoretical shear and bending stresses with experimental results for a 45° sweptback box beam loaded by constant tip shear and constant tip torque loads. The

simplified method of minimum potential energy and the Wittrick and Thompson method were used for the calculations of the theoretical stresses. The stresses were calculated for the shear and bending stresses in a 45° sweptback box beam tested by the National Advisory Committee for Aeronautics, hereafter referred to as the NACA beam. The experimental and theoretical results for this beam under the condition of a constant tip shear load were compared with the theoretical and experimental results obtained in a test of a similar beam at Massachusetts Institute of Technology, hereafter called the MIT beam. The other methods which have been described were considered for the calculations, but because of the extremely lengthy calculations involved in these methods it was decided that it was not practical to include them in this thesis.

CHAPTER II

METHODS USED FOR ANALYSIS

The Simplified Method of Minimum Potential Energy for the Condition of a Shear Load Applied at the Tip

The simplified method of minimum potential energy was described in the introduction of this thesis. A complete derivation of this method is not given here as it has been completely derived in ref. 8. The basic equations are given, however, and also the expressions which were used for the sample calculations in Appendix I.

The wing is considered in two parts, as is explained in ref. 8, as shown in Fig. 1 of Appendix II. The portion of the wing outboard of Section A-B is analyzed on the assumption that it is attached to an elastic support at Section A-B. A simplified analysis is made of the triangular section inboard of Section A-B to determine the properties of the elastic support. Then the two sections are joined by writing an equation of equilibrium which requires the warping across the Section A-B to be equal in each. A free body diagram for the loading configuration under consideration (9) in this section is shown in Fig. 2.

The expression for the total internal strain energy of the outer section is (10),

$$U_i = 1/2 \int_o^{\ell} \left\{ \frac{2A_4 \sigma_4^2}{E} + \frac{2A_1 \sigma_1^2}{E} + \frac{2 \tau_c^2 b t_c}{G} + \frac{\tau_{fw}^2 h t_w}{G} + \frac{\tau_{rw}^2 h t_w}{G} \right\} dx \quad (1)$$

and the potential energy of the external loads is (11),

$$U_e = - Pv(\ell) + 2R_1 u_1(0) \quad (2)$$

where,

$v(\ell)$ Vertical deflection of the center line of the beam at the tip, station ℓ, where the load is applied.

$u_1(0)$ the deformation in the x direction of flange 1 at the juncture of the inner and outer sections, station 0.

The expression for the total strain energy of the inner section including the web and covers is (12),

$$U_i = 1/2 \int_o^b \left(\frac{2A_1 \sigma_1^2}{E} + \frac{2 \tau_c^2 t_c x}{G} + \frac{\tau_{fw}^2 t_w h}{G} \right) dx \quad (3)$$

and the potential energy of the external loads is (13),

$$U_e = - 2R_1 u_1(b) \quad (4)$$

In the analysis of ref. 8 the following expressions were derived for the stresses (14):

$$\frac{\sigma_1}{P} = \frac{R_1}{A_1} \left\{ \cosh \beta x - \frac{\sinh \beta x}{\tanh \beta \ell} \right\} + \frac{\ell}{2hA_4} \left\{ \frac{\sinh \beta x}{\tanh \beta \ell} - \cosh \beta x \right\} + \frac{\ell - x}{2hA_4} \quad (5)$$

$$\frac{\sigma_4}{P} = \frac{R_1}{A_1}\left\{\frac{\text{Sinh } \beta x}{\text{Tanh } \beta \ell} - \text{Cosh } \beta x\right\}$$

$$+ \frac{\ell A_1}{2hA_4^2}\left\{\text{Cosh } \beta x - \frac{\text{Sinh } \beta x}{\text{Tanh } \beta \ell}\right\}$$

$$+ \frac{(2A_4 - A_1)(\ell - x)}{2hA_4^2} \tag{6}$$

$$\frac{\sigma_2}{P} = -\frac{\sigma_1}{P} \tag{7}$$

$$\frac{\sigma_3}{P} = -\frac{\sigma_4}{P} \tag{8}$$

$$\frac{\tau_c}{P} = \frac{1}{2t_c}\left[A_1 \frac{d\left(\frac{\sigma_1}{P}\right)}{dx} + \frac{1}{2h}\right] \tag{9}$$

$$\frac{\tau_{fw}}{P} = -\frac{t_c}{t_w}\frac{\tau_c}{P} + \frac{1}{2ht_w} \tag{10}$$

$$\frac{\tau_{rw}}{P} = -\frac{t_c}{t_w}\frac{\tau_c}{P} - \frac{1}{2ht_w} \tag{11}$$

The value for R_1 in the expression for $\frac{\sigma}{P}$ is obtained by analyzing the inner section and writing an equation of continuity joining the inner and outer sections.

Analysis Including Inner Section Shear Lag Effects.--For the analysis of the inner section including shear lag effects (15) the unknown internal force R_1 is obtained by equating,

$$u_1(0) = -\left(\frac{2\coth \beta\ell}{\beta A_1 E}\right) R_1 + \left(\frac{\ell}{\beta A_4 Eh} \coth \beta\ell\right) P \tag{12}$$

for the outer box to,

$$u_1(b) = \sum_{j=1}^{n} c_j b^j \tag{13}$$

for the inner box. Fig. 3 shows a diagram of the inner section.

For the sweptback wing outboard section (16)

$$\beta^2 = \frac{8G}{A_1 E\left(\frac{b}{t_c} + \frac{h}{t_w}\right)} \tag{14}$$

$$a_o^2 = \frac{Gt_c}{A_1 E} \tag{15}$$

$$b_o^2 = \frac{2Gt_w}{hA_1 E}$$

$$C_{j+1} = \frac{a_o^2 C_j + b_o^2 C_{j-1}}{j(j+1)} \tag{17}$$

Expanding Eq. (13) to obtain $u_1(x)$,

$$u_1(x) = \left\{C_1 x + C_2 x^2 + C_3 x^3 + C_4 x^4 + C_5 x^5 + ..\right\} \tag{18}$$

Utilizing the boundary conditions (17)

$$u_1(0) = 0 \; ; \quad A_1 E \frac{du_1(b)}{dx} = R_1 \tag{19}$$

C_1 may be obtained in terms of R_1.

Then $x = b$ is substituted into Eq. (18) and, for continuity, u_1 (0) outboard, Eq. (12), is equated to u_1 (b) inboard, Eq. (18), to solve for R_1.

The normal and shear stresses in the outboard section may now be computed for the case including inner section shear lag effects by substituting the value of R_1 calculated above into Eqs. (5) to (11).

Analysis Neglecting Inner Section Shear Lag Effects. -- For the analysis neglecting inner section shear lag effects the deformation of flange

number one in the x direction becomes, from elementary theory, simply (18),

$$u_1 = \frac{R_1}{A_1 E} \quad x \tag{20}$$

In this case x is set equal to b. The equation of continuity requires that Eq. (12) be equated to Eq. (20). The value for R_1 obtained by this method is substituted into Eq. (5) to (11) to solve for the normal and shear stresses in the outboard section.

The Simplified Method of Minimum Potential Energy for the Condition of a Torque Load Applied at the Tip

For the case of a constant torque load applied in the plane of the rib at the tip of the box beam, as shown in Fig. 4, the simplified minimum potential energy method yields the following expressions for the shear stresses in the webs and covers (19):

$$\tau_c = \frac{1}{2t_c}\left(\frac{T}{bh}\right) = \frac{T}{2t_c bh} \tag{21}$$

$$\tau_{fw} = \tau_{rw} = -\frac{t_c}{t_w}\tau_c + \frac{T}{t_w bh} = \frac{T}{2t_w bh} \tag{22}$$

The Wittrick and Thompson Method

The method derived by Wittrick and Thompson in refs. 5 and 6 has been described in the introduction of this thesis. This method yields the following equations for the shear stresses in the webs and covers and the direct stress parallel to the stringers in the covers (20):

$$\tau_{rw} = \tau_{fw} = \frac{T - M_y \tan \alpha}{2t_w bh} \tag{23}$$

$$\tau_c = \frac{T - M_y \tan \alpha}{2t_c bh} + f_2 \cot \phi \tag{24}$$

$$f_2 = -\frac{\sin \phi \cos \phi}{2bhGKt_c} \left[T - M_y \tan \alpha - \frac{\left\{ T + \frac{M_y}{\sin \alpha \cos \alpha} \left(2\cos^2 \phi \, \frac{2G}{E'} \sin^2 \phi - \sin^2 \alpha \right) \right\} \left(\frac{\ell_1 + \ell_3}{\ell_1} \right)^2}{L} \right] \tag{25}$$

where,

$$L = \frac{4}{3 \ell_1^2} \left\{ \ell_1^2 + \ell_3^2 + \ell_1 \ell_3 \right\} + K \sin \phi \left[4E \left\{ k_1 + k_3 \frac{\ell_3^2}{\ell_1^2} \right\} \right] + \frac{2E' \ell_1}{3 \ell_2 t_2} \left\{ t_1 + t_3 \frac{\ell_3^3}{\ell_1^3} \right\} + \frac{4Et_s}{3t_2} \sin \phi \left\{ \frac{\ell_1^2 + \ell_3^2 + \ell_1 \ell_3}{\ell_1^2} \right\} \tag{26}$$

For the case of a sweptback box beam with ribs parallel to the airstream, a rectangular cross section, and loaded only by a torque load these equations reduce to,

$$\tau_{rw} = \tau_{fw} = \frac{T}{2t_w bh} \tag{27}$$

$$\tau_c = \frac{T}{2t_c bh} + f_2 \cot \phi \tag{28}$$

$$f_2 = - \frac{T}{2t_c bh} \left[\frac{\sin\alpha \cos\alpha}{\sin^2\alpha + \frac{G}{E'} \cos^2\alpha} - \frac{\sin\alpha \cos\alpha}{L' \left(\sin^2\alpha + \frac{G}{E'} \cos^2\alpha \right)} \right] \tag{29}$$

where,

$$L' = 1 + \left(\sin^2\alpha + \frac{G}{E'} \cos^2\alpha \right) \left\{ \frac{E' \ell_1 \cos\alpha}{6G \ell_2} \left(\frac{2t_w}{t_c} \right) + \frac{E \cos\alpha}{G} \left(2k_1 + \frac{t_s \cos\alpha}{t_c} \right) \right\} \tag{30}$$

If the ribs are perpendicular to the spars ϕ is 90° and the equation for the shear stress in the covers further reduces to,

$$\tau_c = \frac{T}{2t_c bh} \tag{31}$$

It may be seen that these equations for the shear stresses reduce to the same equations used for calculating the shear stresses in an unswept box beam.

CHAPTER III

EQUIPMENT

The Massachusetts Institute of Technology Test Beam.--The box beam tested at MIT was a stressed skin, two spar wing, sweptback at 45°. The planform and cross section of this beam are illustrated by Fig. 5. The spars were parallel, of equal length, and of constant cross section. The spar flanges were made up of two 3/4 x 3/4 x 1/8 24ST extruded angles, back to back, and separated by the spar webs. Three equally spaced 1/2 x 1/2 x 1/16 24ST extruded angles were used as longitudinal stiffeners on the upper skin and three on the lower skin. The webs and ribs were constructed of 0.051 inch 75ST sheet. The upper and lower skins were constructed of 0.032 inch 75ST sheet. The cross section perpendicular to the spars was a rectangular box 12 inches wide and 6 inches deep. Six solid ribs parallel to the air-stream were spaced at 8.484 inch intervals along a line normal to the airplane center line.

The overall length of the beam measured parallel to the spars was 60 inches. The root section of the box beam, inboard of the inner rib, was built around a heavy steel attachment fitting to approximate a fixed end condition. This is illustrated by Fig. 5.

A single Black Hawk hydraulic jack with a one ton capacity was used to load the wing. The point of application of the load was located precisely by inserting a knife edge between the jack pad and the wing.

Electric strain gages were located at 43 points on the flanges and webs and these were used to obtain the stresses. The normal stresses were measured by gages, mounted longitudinally in pairs on opposite sides of the flanges, along the flanges. The shear stresses were measured by gages mounted at 45° to the vertical on only one side of the webs. The majority of the gages were mounted in the vicinity of the root. The vertical deflections were measured at 10 points by Ames dial gages attached to a fixed supporting structure above the wing (21).

The National Advisory Committee for Aeronautics Test Beam.--The swept-back box beam tested by the NACA at Langley Field, Virginia, consisted of two stressed skin, two spar box beams, sweptback at right angles to each other. These beams were joined by and continuous with a short rectangular carry-through bay. The planform and cross section of this beam are illustrated by Fig. 6. The material used in the construction of this beam was 24ST aluminum alloy except for the ribs. The ribs were solid rectangular steel sheets with a 90° bend at each edge forming flanges for attachment to the spars and covers. Ribs 2, 3, 4, and 5 were 3/32 inch thick and the other ribs were 1/8 inch thick. The spar flanges were $1\frac{1}{4} \times 1\frac{1}{4} \times 1/8$ inch angles. The webs were 0.078 inch thick, and the covers were 0.050 inch thick. Thirteen equally spaced $3/4 \times 3/4 \times 1/16$ inch angles were used as longitudinal stiffeners on the upper skin and thirteen on the lower skin. The cross section perpendicular to the spars was a rectangular box 30 inches wide and 7.05 inches deep.

The beam was supported by steel rollers, with axes parallel to the center line of the carry-through bay, at the corners of the carry-through bay. The loads were applied at the tips of the sweptback beams by means of hand-operated winches. The loads were transferred from the winches to horizontal steel I-beams and then to the tip ribs.

All strains were measured by Tuckerman optical strain gages. All stringer strains and strains at a 45° angle to the spar-web center lines were measured using 2-inch gage lengths. All other strains were measured using 1-inch gage lengths. The smallest divisions of the gages used to measure stringer strains were 0.000004 in./in. The smallest divisions of the gages used to measure the strains at a 45° angle to the spar-web center lines were 0.000002 in./in. The smallest divisions of the 1-inch gage lengths were 0.000004 in./in. The spar deflections were measured by means of dial gages. The smallest divisions of these gages were 0.001 inch in the bending tests and 0.0001 inch in the torsion tests. The forces exerted by the winches were measured by means of dynamometers accurate to within 10 pounds of the exact values (22).

CHAPTER IV

METHODS OF LOADING THE SWEPTBACK BEAMS

The methods of applying the shear loads to the MIT beam and the NACA beam were different in that the MIT beam was loaded by applying the shear load at a point midway between stations 2 and 3 while the shear loads applied to the NACA beam were applied through steel I-beams which were fastened to the tip ribs by brackets at each end of the ribs. Fig. 7 illustrates the method by which the shear loads were applied to the NACA beam. The loads were applied to the NACA beam both symmetrically and antisymmetrically. For the test in which the beam was symmetrically loaded, the loads were applied vertically downward at each tip. For the test in which the beam was loaded antisymmetrically the load was applied vertically downward at one tip and vertically upward at the other tip.

The NACA beam was also tested under the conditions of constant torque loadings applied at the tips. An illustration of the method by which the torque loadings were transferred to the beam is shown in Fig. 8. These loads were also applied both symmetrically and antisymmetrically. For the symmetrically loaded condition both torque loads were applied in the same direction. For the antisymmetrically loaded condition the torque loads were applied in opposite directions at the tips.

CHAPTER V

DISCUSSION

It was found by the NACA that when symmetrical shear loads were applied to the tips of the beam which they tested the normal stress in the rear spar at the root was approximately 1.4 times the stress predicted by the elementary $\frac{Mc}{I}$ formula. The vertical shear stress in the rear spar web at the root was about $1\frac{1}{3}$ times the vertical shear stress at the tip. When symmetrical torque loads were applied the shear stresses in the webs and covers in the vicinity of the root showed a marked decrease. It was also found that normal stresses in the stringers of about half the magnitude of the shear stress $\frac{T}{2At}$ were produced at the root as a result of the restraint against cross-sectional warping provided by the triangular bay.

For the case of antisymmetrical shear loads applied to the tips of the beam, it was determined that the normal stress in the rear spar at the root was 1.6 times the $\frac{Mc}{I}$ stress. The vertical shear stress in the rear spar web at the root, for this case, was over 1.6 times the vertical shear stress at the tip. When antisymmetrical torque loads were applied there was an appreciable decrease in the shear stresses in the covers and webs in the vicinity of the root. It was found that longitudinal stringer stresses of about half the magnitude of the shear stress $\frac{T}{2At}$ were produced at the root also.

In the simplified method of minimum potential energy the assumption is made that the root of the box beam is rigidly supported. This

assumption is not completely justified in the case of the NACA beam as there is some distortion of the carry-through bay. If there were no distortion of this bay the stresses should be the same for symmetrical loading as for antisymmetrical loading. The NACA test more nearly approximates the stress conditions that would be encountered in an airplane wing as there is always some distortion of the fuselage or other wing supporting structure when the wing is under load.

The simplified method of minimum potential energy including shear lag yields results which are unconservative for the normal stresses in the spar flanges in the vicinity of the root of the NACA beam. When shear lag is neglected the theoretical results for the normal stresses in the rear spar flanges are conservative for the case of symmetrical loading and unconservative for the case of antisymmetrical loading. This is illustrated by the curves in Fig. 9. In Fig. 10 the rear spar flange stresses in the MIT and the NACA beams are plotted against per cent of the semi-span as measured along the leading edge of the beam. This figure illustrates that the theoretical results, both including shear lag and neglecting shear lag, are conservative for the rear spar stresses in the MIT beam.

In Fig. 11 the shear stresses in the webs are plotted against the station along the span for the NACA beam. This figure shows that the results using the simplified method of minimum potential energy tend to become unconservative for the shear stresses in the vicinity of the root when shear lag effects are included in the theory. The results are conservative for the rear web stresses and unconservative for the front web stresses when shear lag effects are neglected. The elementary

$\frac{1}{2ht_w}$ formula, for the shear stresses in the webs caused by a unit shear load, yields acceptable results for the stresses outboard of a section one chord width from the root. The unit load form is used for both the NACA and the MIT beams so the results may be compared for these beams when both are under the same load condition. The theoretical and experimental results for the shear stresses in the rear spar webs, caused by unit shear loads applied at the tips, of the MIT and NACA beams have been plotted in Fig. 12. Here, the experimental shear stresses in the webs of the NACA beam followed the same general trend as the shear stresses in the webs of the MIT beam. For the case of antisymmetrically placed shear loads the rear spar web shear stresses in the NACA beam increased very rapidly in magnitude in the vicinity of the root. At the 31 per cent station, for example, corresponding to 6.8 inches from the rear spar root, the shear stresses in the webs for antisymmetrical loading were 1.2 times as large as for the symmetrically loaded condition.

In the description of the methods of analysis it was shown that both the simplified method of minimum potential energy and the Wittrick and Thompson method reduce to the $\frac{T}{2At}$ formula, as for an unswept box beam, for the case of a sweptback box beam having its ribs perpendicular to the spars and loaded by a constant torque load. Figs. 13 and 14 illustrate the comparison of the experimentally determined shear stresses in the webs and covers of the NACA beam with the stresses calculated by the $\frac{T}{2At}$ formula. Fig. 13 shows that the shear stresses in the covers in the vicinity of the root are higher for the symmetrically loaded condition than for the antisymmetrically loaded condition. These figures indicate that conservative results will be obtained if the $\frac{T}{2At}$ formula

is used to calculate the shear stresses in the webs and covers for the condition of a constant torque loading.

The box beam tested at MIT had ribs which were parallel to the root section and the NACA beam had ribs which were perpendicular to the spars. Barfoot (23) stated that for the same number of ribs the torsional rigidity of a sweptback box beam is far greater when the bulkheads, or ribs, are perpendicular to the spars than when they are parallel to the root section. This probably explains, at least in part, the fact that in the MIT tests the theoretical results compared more conservatively with the experimentally determined values for the stresses than in the NACA tests.

A search was made of the literature in an attempt to find an analogy between sweptback plate and sweptback box beam theory. No direct analogy could be found in the literature and none is readily apparent. Several of the references on sweptback plate theory are cited in the bibliography.

CHAPTER VI

CONCLUSIONS

The simplified method of minimum potential energy neglecting inner section shear lag effects gives conservative results for both the shear and normal stresses caused by symmetrical loading but gives unconservative results for the normal stresses in the stringers caused by antisymmetrical loading.

The simplified method of minimum potential energy including inner section shear lag effects does not give conservative results for the root stresses for all cases. Thus, if this method is used in preliminary design it must be used with caution.

The Wittrick and Thompson method is satisfactory only for predicting the stresses remote from the root in sweptback box beams as it does not take into account the variation of stresses in the vicinity of the root.

The elementary formulas for an unswept box beam give conservative results for the stresses in the front spar flanges and spar webs and may also be used to predict the stresses remote from the root in the rear spar flanges and webs of sweptback box beams.

A carry-through bay creates the effect of an elastic support at the root of a sweptback box beam and allows a very rapid buildup of the normal stresses in the rear spar flanges in the vicinity of the root for the case of antisymmetrical loading. A rigid support at the root does not allow such a rapid buildup of these stresses in the vicinity of the root.

CHAPTER VII

RECOMMENDATIONS

It is highly recommended that more experimental data on the stresses in sweptback box beams be obtained. It is thought that if sweptback box beams of several different degrees of sweep, several different aspect ratios, and of both straight and tapered planform were tested and the experimental results for the stresses were plotted that a much better idea of the general trend of stress variation in these beams would be gained. The methods developed so far for the calculations of these stresses should be compared with the experimental results obtained in the proposed tests as there is a lack of experimental evidence to substantiate the theories which have been developed.

It is also recommended that an attempt be made to derive a method for the calculations of stresses in a sweptback box beam having thick webs and thick cover skins. In this type of construction the webs and covers take a considerable portion of the bending stresses as well as the shear stresses. Under such conditions, lumping all the bending material into four spar cap areas may not be a satisfactory approximation. If such were the case, the basic theory might have to be revised.

BIBLIOGRAPHY

Literature Cited

(1) S. Levy, "Computation of Influence Coefficients for Aircraft Structures With Discontinuities," Journal of the Aeronautical Sciences, 14:547-560, October, 1947.

(2) R. L. Bisplinghoff and Arthur Lang, "An Investigation of Deformations and Stresses in Sweptback and Tapered Wings With Discontinuities," Massachusetts Institute of Technology Aero-Elastic and Structures Report, Contract No. a(s)-8790, July, 1949, p. 3.

(3) Ibid., pp. 133-140.

(4) George Zender, Richard Heldenfels, and Charles Libove, "Stress and Distortion Analysis of a Swept Box Beam Having Bulkheads Perpendicular to the Spars, "U.S. National Advisory Committee for Aeronautics, Technical Note No. 2232, November, 1950.

(5) W. H. Wittrick, "Preliminary Analysis of a Highly Swept Cylindrical Tube Under Torsion and Bending, "Council for Scientific and Industrial Research, Aeronautical Research Report, ACA-39, Victoria, Australia, May, 1948, 23 p.

(6) W. H. Wittrick and J. J. Thompson, "The Stresses in Certain Cylindrical Swept Tubes Under Torsion and Bending," Council for Scientific and Industrial Research, Aeronautical Research Report, ACA-43, Victoria, Australia, January, 1949, 20 p.

(7) J. Hadji-Argyris and P. C. Dunne, "The General Theory of Cylindrical and Conical Tubes Under Torsion and Bending Loads," Journal of the Royal Aeronautical Society, 51:199-269, Parts I-IV, February, 1947, 51:757-784, Part V, September, 1947, 51: 884-930, Part V concluded, November, 1947.

(8) Bisplinghoff and Lang, op. cit., pp. 7-27.

(9) Ibid., p. 8.

(10) Ibid., p. 9.

(11) Ibid., p. 9.

(12) Ibid., p. 20.

(13) Loc. cit.

(14) Ibid., p. 25.

(15) Ibid., pp. 20-26.

(16) Ibid., pp. 22-24.

(17) Ibid., p. 21.

(18) Ibid., p. 22.

(19) Ibid., p. 18.

(20) Wittrick and Thompson, op. cit., p. 8.

(21) Bisplinghoff and Lang, op. cit., pp. 3-4, 45-50.

(22) Zender and Libove, op. cit., pp. 3-4.

(23) J. E. Barfoot, "Design of Swept-back Wings," Aero Digest, 54: 55-57, 134-135, June, 1947, p. 55.

Other References

Barton, M. V., "Finite Difference Equations for the Analysis of Thin Rectangular Plates with Combinations of Fixed and Free Edges," Defense Research Laboratory, DRL-175, August, 1948.

DeGroff, H. M., "Experimental Investigation of the Effect of Sweep Upon the Stress and Deflection Distribution in Cantilever Plates of Constant Chord and Thickness," Air Force Technical Report No. 5761-3, June, 1949.

Fung, Y. C., "Stress and Deflection Analysis of Swept Plates," Air Force Technical Report No. 5761-2, February, 1950.

Hill, G. T. R., "The Nature of the Distortion of Sweptback Wings," Journal of the Royal Aeronautical Society , London, March, 1948.

Jensen, V. P., "Analysis of Skew Slabs," University of Illinois, Engineering Experiment Station, Bulletin No. 332, Vol. XXXIX, No. 3, September, 1941.

Rand, Thorkild, "An Approximation Method for the Calculation of the Stresses in Sweptback Wings," Journal of the Aeronautical Sciences, 18:61-63, January, 1951.

Sechler, E. E., "An Initial Approach to the Overall Structural Problems of Swept Wings Under Static Loads," Institute of the Aeronautical Sciences, Preprint No. 257, December, 1949.

"Sweepback Effects on Box Beam Stresses," Aviation Week, 52:20-22, April 3, 1950.

Zender, George, and Charles Libove, "Stress and Distortion Measurements in a 45° Swept Box Beam Subjected to Bending and Torsion," U.S. National Advisory Committee for Aeronautics, Technical Note No. 1525, March, 1948.

Zender, George, and Richard Heldenfels, "Stress and Distortion Measurements in a 45° Swept Box Beam Subjected to Antisymmetrical Bending and Torsion," U.S. National Advisory Committee for Aeronautics, Technical Note No. 2054, April, 1950.

APPENDIX I

SAMPLE CALCULATIONS

The Elementary Formulas for the Flange and Web Stresses as for an Unswept Box Beam.--For the case of a shear load applied at the tips of the NACA beam, applying the elementary formulas gives the following results:

For the normal flange stresses;

$$\sigma = \frac{Mc}{I}$$

$$I = 4(1.815)\,(3.525)^2 = 90.23 \text{ in.}^4$$

$$\frac{\sigma}{P} = \frac{3.525x}{90.23} = 0.0391x$$

For the web shear stress;

$$\tau_w = \frac{V}{2ht_w}$$

$$\frac{\tau_w}{V} = \frac{1}{2(7.05)\,(0.078)} = 0.915$$

Analysis Including Inner Section Shear Lag Effects.--For the 45° swept-back wing outboard section,

$$\beta^2 = \frac{8G}{A_1E\left(\frac{b}{t_c} + \frac{h}{t_w}\right)} = \frac{8(4)\,(10^6)}{(1.815)\,(10.5)\,(10^6)\left(\frac{30}{0.050} + \frac{7.05}{0.078}\right)}$$

$$\beta^2 = 0.002432$$

$$\beta = 0.04932$$

From Eq. (12),

$$U_1(0) = -\frac{2}{0.04932(1.815)\quad(10.5)\quad(10^6)}\,R_1 + \frac{88.75P}{0.04932(1.815)\quad(10.5)\quad(10^6)\quad(7.05)}$$

$$U_1(0) = -2.1279\times10^{-6}R_1 + 13.3934\times10^{-6}P$$

$$a^2 = \frac{Gt_c}{A_1E} = \frac{4(10^6)\quad(0.050)}{1.815(10.5)\quad(10^6)} = 0.010494$$

$$b^2 = \frac{2Gt_w}{hA_1E} = \frac{2(4)\quad(10^6)\quad(0.078)}{7.05(1.815)\quad(10.5)\quad(10^6)} = 0.004644$$

$$C_{j+1} = \frac{a_o\,{}^2C_j + b_o\,{}^2C_{j-1}}{j(j+1)}$$

$$C_2 = 0.005247C_1$$

$$C_3 = 0.000783177C_1$$

$$C_4 = 0.2715477\times10^{-5}C_1$$

$$C_5 = 1.83278\times10^{-7}C_1$$

$$C_6 = 0.484466\times10^{-9}C_1$$

$$C_7 = 2.038641\times10^{-11}C_1$$

$$C_8 = 0.439963\times10^{-13}C_1$$

$$C_9 = 1.321336\times10^{-15}C_1$$

$$C_{10} = 0.242428\times10^{-17}C_1$$

$$C_{11} = 0.560157\times10^{-19}C_1$$

$$C_{12} = 0.897438\times10^{-22}C_1$$

$$C_{13} = 1.673581\times10^{-24}C_1$$

From Eq. (18),

$$U_1(x) = C_1 \{ x + 0.005247x^2 + 0.000783177x^3 + 0.2715477x10^{-5}x^4 + 1.832785(10^{-7})x^5 + 0.484466(10^{-9})x^6 + 2.038641(10^{-11})x^7 + 0.439963(10^{-13})x^8 + 1.321336(10^{-15})x^9 + 0.242428(10^{-17})x^{10} + 0.560157(10^{-19})x^{11} + 0.897438(10^{-22})x^{12} + 1.673581(10^{-24})x^{13} \ldots \}$$

From the boundary conditions given by Eq. (19),

$$C_1 = 0.01127(10^{-6})R_1$$

Putting x = 30 inches,

$$U_1(30) = 0.01127(10^{-6})R_1 \{ 30 + 4.7223 + 21.145779 + 2.199536 + 4.453668 + 0.353176 + 0.445851 + 0.028866 + 0.026008 + 0.001432 + 0.000992 + 0.000048 + 0.000027 + \ldots \} = 0.714266(10^{-6})R_1$$

For continuity, $U_1(0)_{\text{Outb'd.}} = U_1(30)_{\text{Inb'd.}}$

$$-2.1279(10^{-6})R_1 + 13.3934(10^{-6})P = 0.714266(10^{-6})R_1$$

$$R_1 = 4.71239P$$

Putting $R_1 = 4.71239P$, M = 0, and T = 0 into Eqs. (5) to (11) and reducing these equations gives the following results for the normal and shear stresses in the outboard section:

$$\frac{\sigma_1}{P} = 0.8715 \{ \text{Sinh}(0.04932x) - \text{Cosh}(0.04932x) \} + 3.4679 - 0.03908x$$

$$\frac{\sigma_4}{P} = 0.8715 \left\{ \text{Cosh}(0.04932x) - \text{Sinh}(0.04932x) \right\} + 3.4679 - 0.03908x$$

$$\frac{\sigma_2}{P} = -\frac{\sigma_1}{P}$$

$$\frac{\sigma_3}{P} = -\frac{\sigma_4}{P}$$

$$\frac{\tau_{fw}}{P} = -0.5001 \left\{ \text{Cosh}(0.04932x) - \text{Sinh}(0.04932x) \right\} + 0.9093$$

$$\frac{\tau_{rw}}{P} = 0.5001 \left\{ \text{Cosh}(0.04932x) - \text{Sinh}(0.04932x) \right\} - 0.9093$$

The above equations have been evaluated for several different stations along the span as illustrated by Tables I, II, III, and IV.

Analysis Neglecting Inner Section Shear Lag Effects. -- The same value for β is used as in the preceding analysis. Eq. (12) is equated to Eq. (20) in which x is set equal to b, 30 inches, to solve for R_1.

$$-2.1279(10^{-6})R_1 + 13.3934(10^{-6})P = 1.5742(10^{-6})R_1$$

$$R_1 = 3.6178P$$

Putting $R_1 = 3.6178P$, $M = 0$, and $T = 0$ into Eqs. (5) to (11) and reducing these equations gives the following results for the normal and shear stresses in the outboard section:

$$\frac{\sigma_1}{P} = 1.4746 \left\{ \text{Sinh}(0.04932x) - \text{Cosh}(0.04932x) \right\} + 3.4679 - 0.03908x$$

$$\frac{\sigma_4}{P} = 1.4746 \left\{ \text{Cosh } (0.04932x) - \text{Sinh } (0.04932x) \right\} + 3.4679 - 0.03908x$$

$$\frac{\sigma_2}{P} = -\frac{\sigma_1}{P}$$

$$\frac{\sigma_3}{P} = -\frac{\sigma_4}{P}$$

$$\frac{\tau_{fw}}{P} = -0.84615 \left\{ \text{Cosh } (0.04932x) - \text{Sinh } (0.04932x) \right\} + 0.9093$$

$$\frac{\tau_{rw}}{P} = -0.84615 \left\{ \text{Cosh } (0.04932x) - \text{Sinh } (0.04932x) \right\} - 0.9093$$

The above equations have been evaluated for several different stations along the span as illustrated by Tables V, VI, VII, and VIII.

The Simplified Method of Minimum Potential Energy for a Constant Torque Load Applied at the Tip. -- For the case of a constant torque load applied at the tips the shear stresses are calculated by substituting into Eqs. (21) and (22) as follows:

$$\tau_c = \frac{1}{2(0.050)} \left(\frac{T}{7.05(30)} \right) = 0.0473T$$

$$\frac{\tau_{fw}}{P} = \frac{\tau_{rw}}{P} = -\frac{0.050}{0.078} (0.0473) + \frac{1}{0.078(30)\quad(7.05)}$$

$$= 0.0303$$

$$\frac{\tau_c}{T} = 0.0473$$

The Wittrick and Thompson Method. -- For the case of a wing having the ribs perpendicular to the spars the Wittrick and Thompson method was

found to reduce to the elementary $\frac{T}{2At}$ stresses as for an unswept box beam. The $\frac{T}{2At}$ stresses are calculated as follows:

$$\frac{\tau_c}{T} = \frac{1}{2At_c} = \frac{1}{2bht_c}$$

$$= \frac{1}{2(30)\ (7.05)\ (0.050)} = \underline{0.0473}$$

$$\frac{\tau_w}{T} = \frac{1}{2At_w} = \frac{1}{2(30)\ (7.05)\ (0.078)}$$

$$= \underline{0.0303}$$

It may be seen that the simplified method of minimum potential energy and the Wittrick and Thompson method both yield the same results for the shear stresses in the webs and covers. These results are the same as the ones which would be obtained if the beam were not sweptback.

Table 1. Sample Calculations Including Inner Section Shear Lag Effects for the Normal Stresses in the Front Spar Flanges at Several Different Span Stations in the Outer Wing Section.

(1) STATION	(2) SINH(0.04932x)	(3) COSH(0.04932x)	(4) (2)-(3)	(5) 0.8715(4)	(6) 0.03908x	(7) 3.4679 + (5) - (6)
0	0	1.0000	-1.0000	-0.8715	0	2.5964
10	0.51344	1.12412	-0.61068	-0.5322	0.3908	2.5449
20	1.15434	1.52726	-0.37292	-0.3250	0.7816	2.3613
30	2.08165	2.30946	-0.22781	-0.1985	1.1724	2.0970
40	3.52589	3.66497	-0.13908	-0.1212	1.5632	1.7835
50	5.84523	5.93016	-0.08493	-0.0740	1.9540	1.4399
60	9.61538	9.66724	-0.05186	-0.0452	2.3448	1.0779
80	25.8762	25.8955	-0.0193	-0.0168	3.1264	0.3247

Table 2. Sample Calculations Including Inner Section Shear Lag Effects for the Normal Stresses in the Rear Spar Flanges at Several Different Span Stations in the Outer Wing Section.

(1) STATION	(2) COSH(0.04932x)	(3) SINH(0.04932x)	(4) (2) - (3)	(5) 0.8715(4)	(6) 0.03908x	(7) 3.4679 + (5)-(6)
0	1.0000	0	1.0000	0.8715	0	4.3394
10	1.12412	0.51344	0.61068	0.5322	0.3908	3.6093
20	1.52726	1.15434	0.37292	0.3250	0.7816	3.0113
30	2.30946	2.08165	0.22781	0.1985	1.1724	2.4940
40	3.66497	3.52589	0.13908	0.1212	1.5632	2.0259
50	5.93016	5.84523	0.08493	0.0740	1.9540	1.5879
60	9.66724	9.61538	0.05186	0.0452	2.3448	1.1683
80	25.8955	25.8762	0.0193	0.0168	3.1264	0.3583

Table 3. Sample Calculations Including Inner Section Shear Lag Effects for the Shear Stresses in the Front Spar Webs at Several Different Span Stations in the Outer Wing Section.

(1) STATION	(2) COSH(0.04932x)	(3) SINH(0.04932x)	(4) (2)-(3)	(5) 0.5001(4)	(6) 0.9093 - (5)
0	1.0000	0	1.0000	0.5001	0.4092
10	1.12412	0.51344	0.61068	0.3054	0.6039
20	1.52726	1.15434	0.37292	0.1865	0.7228
30	2.30946	2.08165	0.22781	0.1139	0.7954
40	3.66497	3.52589	0.13908	0.0696	0.8397
50	5.93016	5.84523	0.08493	0.0425	0.8668
60	9.66724	9.61538	0.05186	0.0259	0.8834
80	25.8955	25.8762	0.0193	0.0097	0.8996

Table 4. Sample Calculations Including Inner Section Shear Lag Effects for the Shear Stresses in the Rear Spar Webs at Several Different Span Stations in the Outer Wing Section

(1) STATION	(2) COSH(0.04932x)	(3) SINH(0.04932x)	(4) (2) - (3)	(5) 0.5001(4)	(6) -0.9093-(5)
0	1.0000	0	1.0000	0.5001	-1.4094
10	1.12412	0.51344	0.61068	0.3054	-1.2147
20	1.52726	1.15434	0.37292	0.1865	-1.0958
30	2.30946	2.08165	0.22781	0.1139	-1.0232
40	3.66497	3.52589	0.13908	0.0696	-0.9789
50	5.93016	5.84523	0.08493	0.0425	-0.9518
60	9.66724	9.61538	0.05186	0.0259	-0.9352
80	25.8955	25.8762	0.0193	0.0097	-0.9190

Table 5. Sample Calculations Neglecting Inner Section Shear Lag Effects for the Normal Stresses in the Front Spar Flanges at Several Different Span Stations in the Outer Wing Section.

(1) STATION	(2) SINH(0.04932x)	(3) COSH(0.04932x)	(4) (2) - (3)	(5) 1.4746(4)	(6) 0.03908x	(7) 3.4679 + (5)-(6)
0	0	1.0000	-1.0000	-1.4746	0	1.9933
10	0.51344	1.12412	-0.61068	-0.9005	0.3908	2.1766
20	1.15434	1.52726	-0.37292	-0.5499	0.7816	2.1364
30	2.08165	2.30946	-0.22781	-0.3359	1.1724	1.9596
40	3.52589	3.66497	-0.13908	-0.2051	1.5632	1.6996
50	5.84523	5.93016	-0.08493	-0.1252	1.9540	1.3887
60	9.61538	9.66724	-0.05186	-0.0765	2.3448	1.0466
80	25.8762	25.8955	-0.0193	-0.0285	3.1264	0.3130

Table 6. Sample Calculations Neglecting Inner Section Shear Lag Effects for the Normal Stresses in the Rear Spar Flanges at Several Different Span Stations in the Outer Wing Section.

(1) STATION	(2) COSH(0.04932x)	(3) SINH(0.04932x)	(4) (2) - (3)	(5) 1.4746(4)	(6) 0.03908x	(7) 3.4679 + (5)-(6)
0	1.0000	0	1.0000	1.4746	0	4.9425
10	1.12412	0.51344	0.61068	0.9005	0.3908	3.9776
20	1.52726	1.15434	0.37292	0.5499	0.7816	3.2362
30	2.30946	2.08165	0.22781	0.3359	1.1724	2.6314
40	3.66497	3.52589	0.13908	0.2051	1.5632	2.1098
50	5.93016	5.84523	0.08493	0.1252	1.9540	1.6391
60	9.66724	9.61538	0.05186	0.0765	2.3448	1.1996
80	25.8955	25.8762	0.0193	0.0285	3.1264	0.3700

Table 7. Sample Calculations Neglecting Inner Section Shear Lag Effects for the Shear Stresses in the Front Spar Webs at Several Different Span Stations in the Outer Wing Section.

(1) STATION	(2) COSH(0.04932x)	(3) SINH(0.04932x)	(4) (2)-(3)	(5) 0.84615(4)	(6) 0.9093 - (5)
0	1.0000	0	1.0000	0.84615	0.0631
10	1.12412	0.51344	0.61068	0.5167	0.3926
20	1.52726	1.15434	0.37292	0.3155	0.5938
30	2.30946	2.08165	0.22781	0.1928	0.7165
40	3.66497	3.52589	0.13908	0.1177	0.7916
50	5.93016	5.84523	0.08493	0.0719	0.8374
60	9.66724	9.61538	0.05186	0.0439	0.8654
80	25.8955	25.8762	0.0193	0.0163	0.8930

Table 8. Sample Calculations Neglecting Inner Section Shear Lag Effects for the Shear Stresses in the Rear Spar Webs at Several Different Span Stations in the Outer Wing Section.

(1) STATION	(2) COSH(0.04932x)	(3) SINH(0.04932x)	(4) (2)-(3)	(5) 0.84615(4)	(6) -0.9093 - (5)
0	1.0000	0	1.0000	0.84615	-1.7555
10	1.12412	0.51344	0.61068	0.5167	-1.4260
20	1.52726	1.15434	0.37292	0.3155	-1.2248
30	2.30946	2.08165	0.22781	0.1928	-1.1021
40	3.66497	3.52589	0.13908	0.1177	-1.0270
50	5.93016	5.84523	0.08493	0.0719	-0.9812
60	9.66724	9.61538	0.05186	0.0439	-0.9532
80	25.8955	25.8762	0.0193	0.0163	-0.9256

APPENDIX II

FIGURES

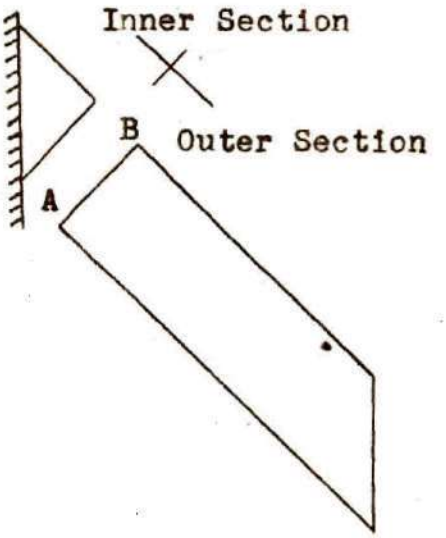

Fig. 1. DIVISION OF SWEPTBACK WING INTO OUTBOARD AND INBOARD SECTIONS

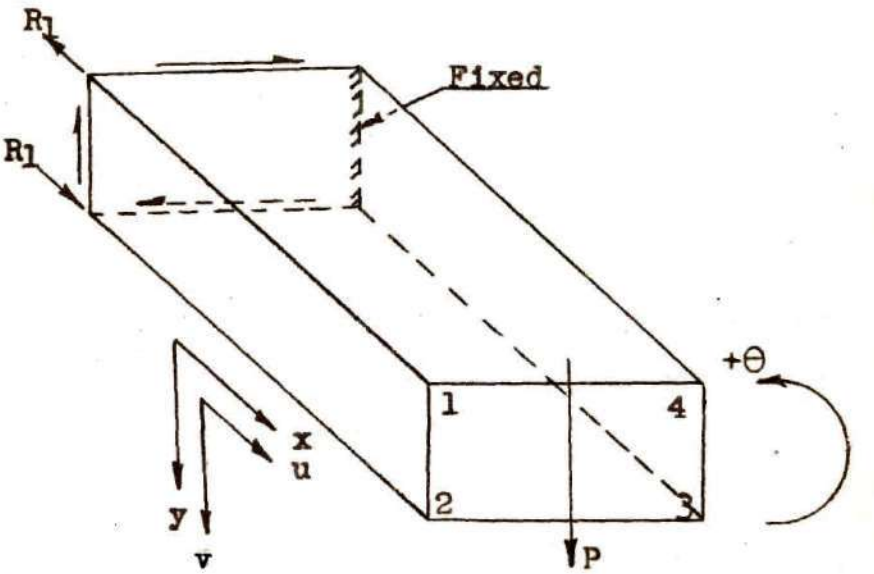

Fig. 2. FREE BODY DIAGRAM OF OUTER SECTION WITH SHEAR FORCE

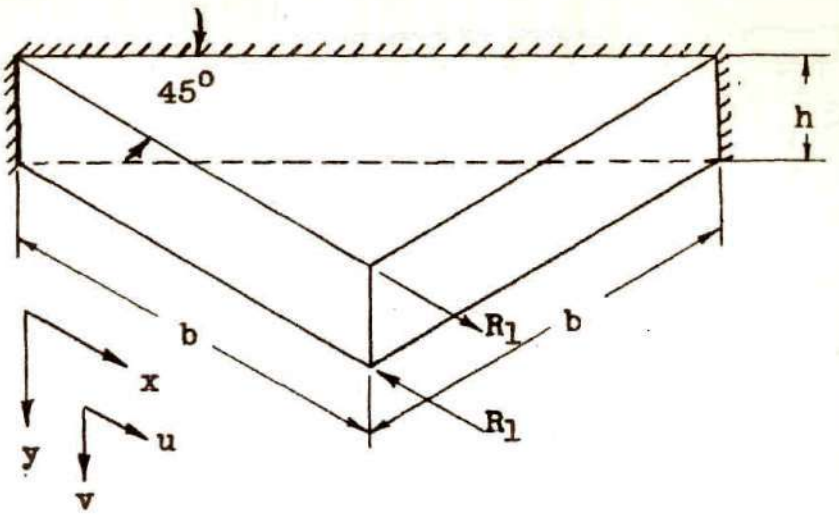

Fig. 3. INNER SECTION AND ITS APPLIED LOADS

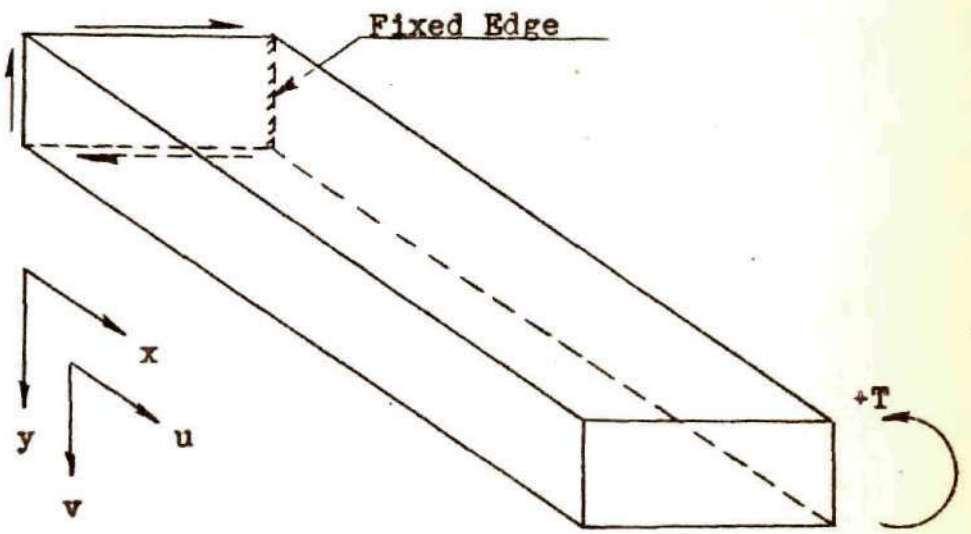

Fig. 4. OUTER WING WITH TORQUE APPLIED

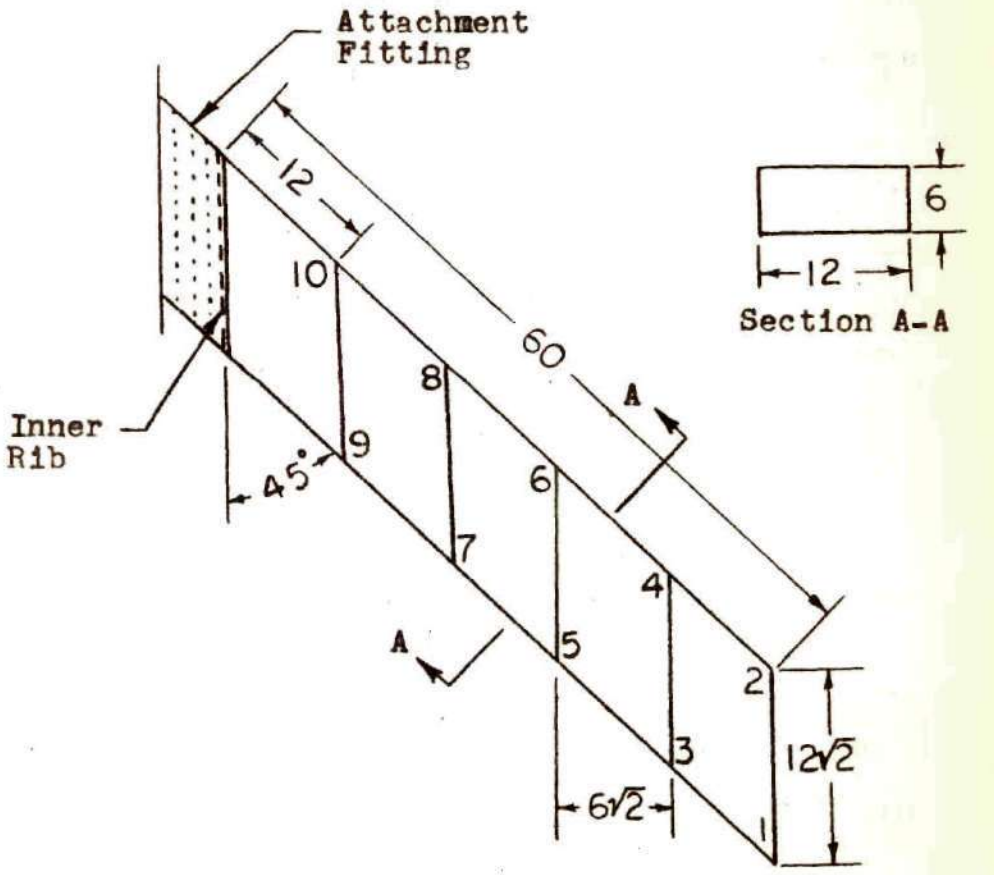

Fig. 5. PLANFORM AND CROSS-SECTION OF THE 45° SWEPT-BACK WING TESTED AT MASSACHUSETTS INSTITUTE OF TECHNOLOGY

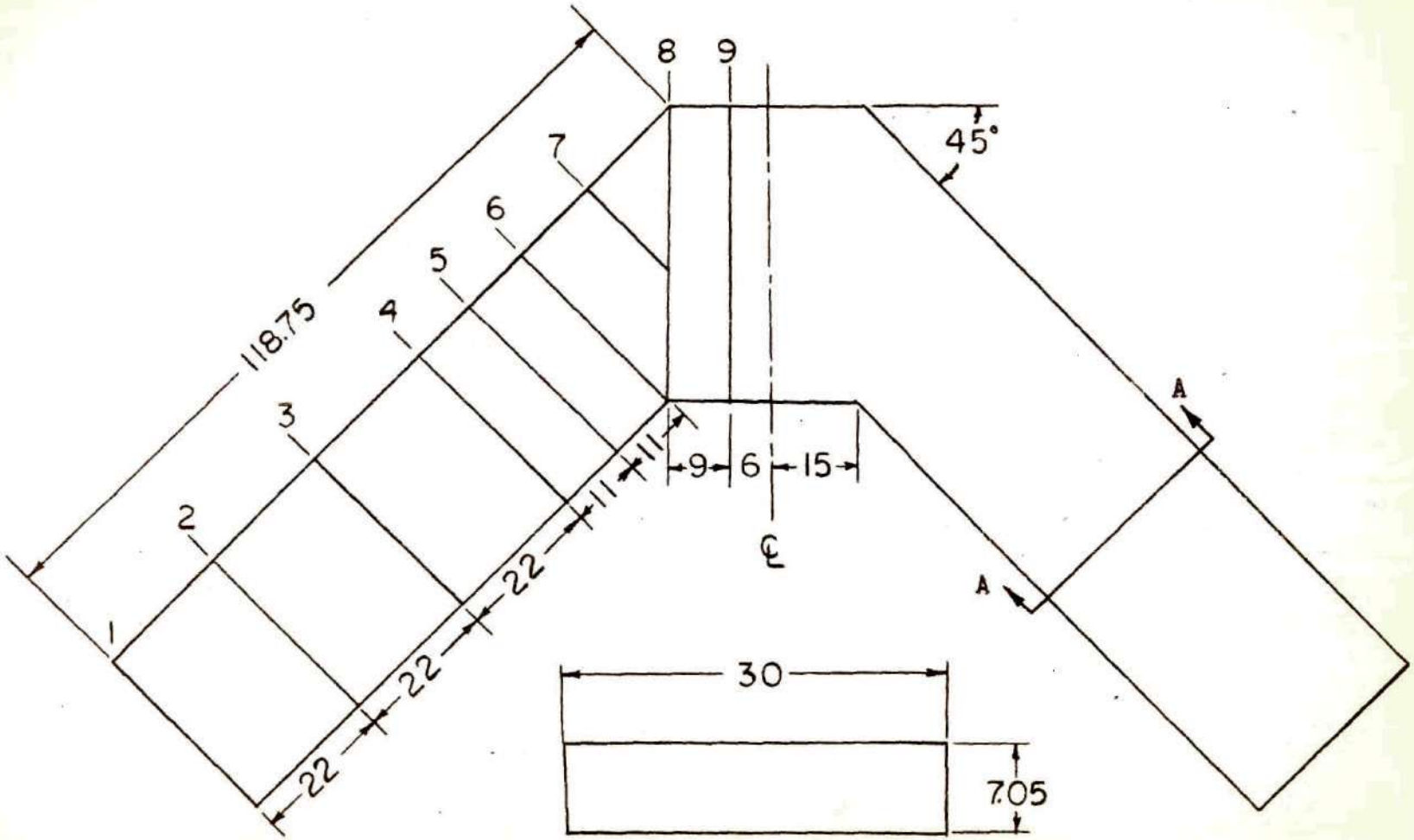

Section A-A

Fig. 6. PLANFORM AND CROSS-SECTION OF THE 45° SWEPTBACK WING SPECIMEN TESTED BY THE NATIONAL ADVISORY COMMITTEE FOR AERONAUTICS

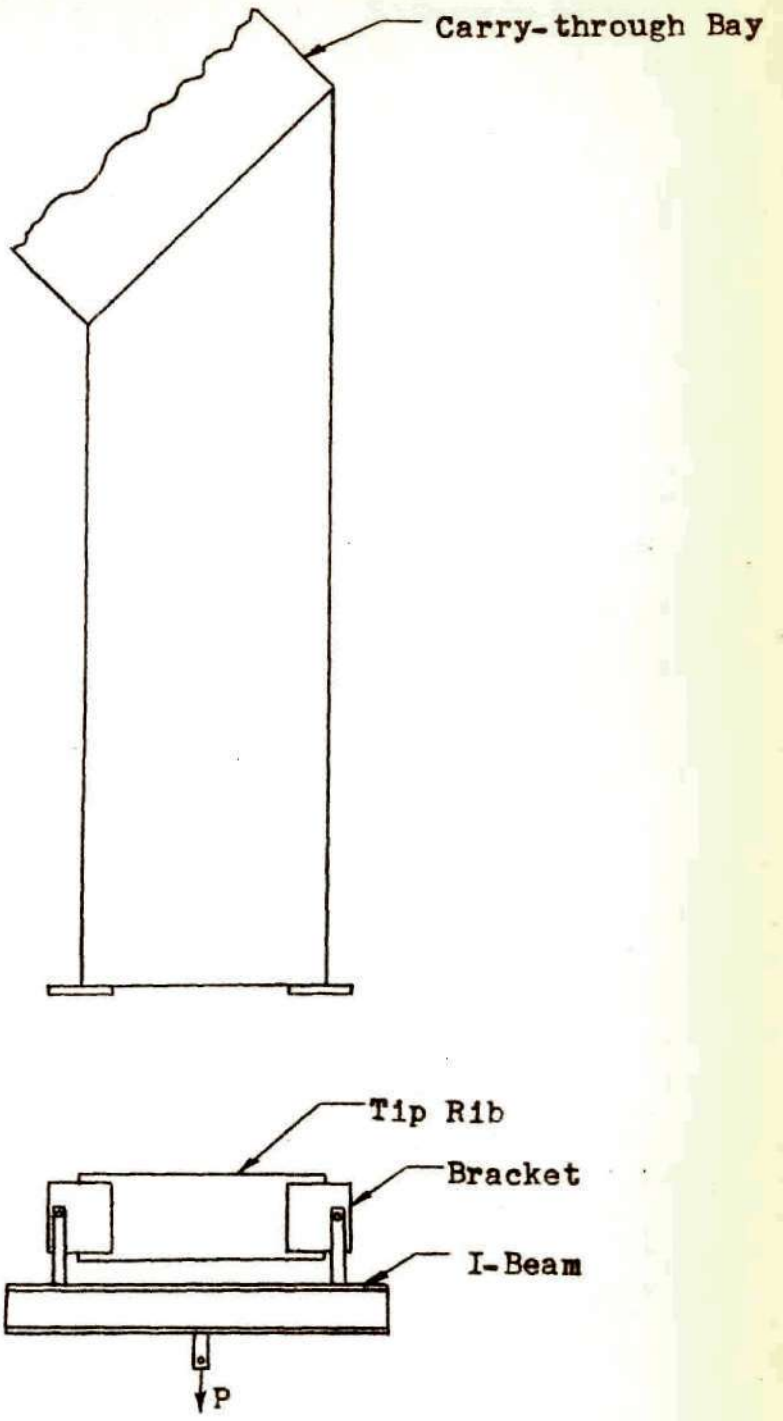

Fig. 7. METHOD OF APPLYING THE SHEAR LOAD TO THE TIP OF THE NACA 45° SWEPTBACK BOX BEAM

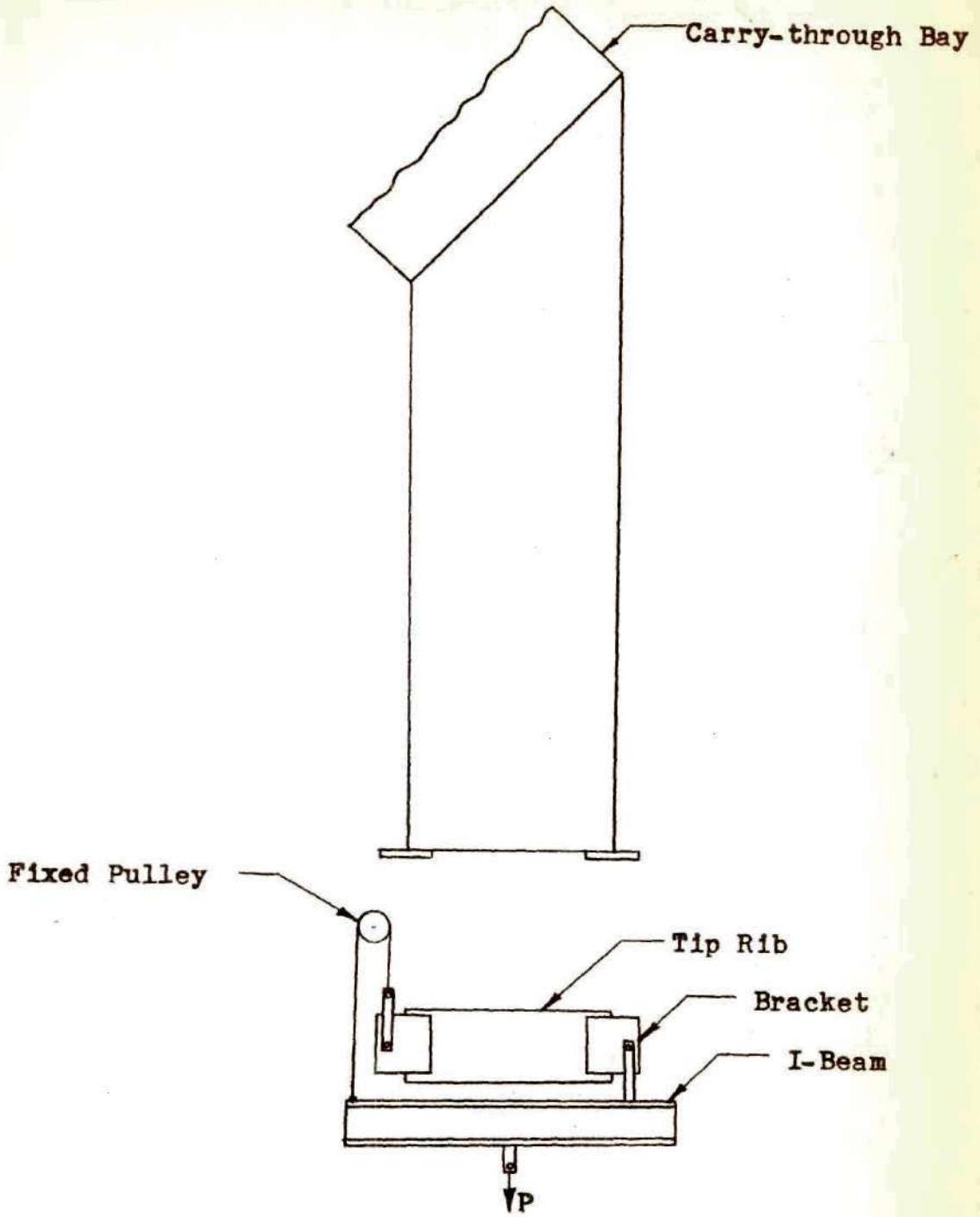

Fig. 8. METHOD OF APPLYING THE TORQUE LOAD TO THE TIP OF THE NACA 45° SWEPTBACK BOX BEAM

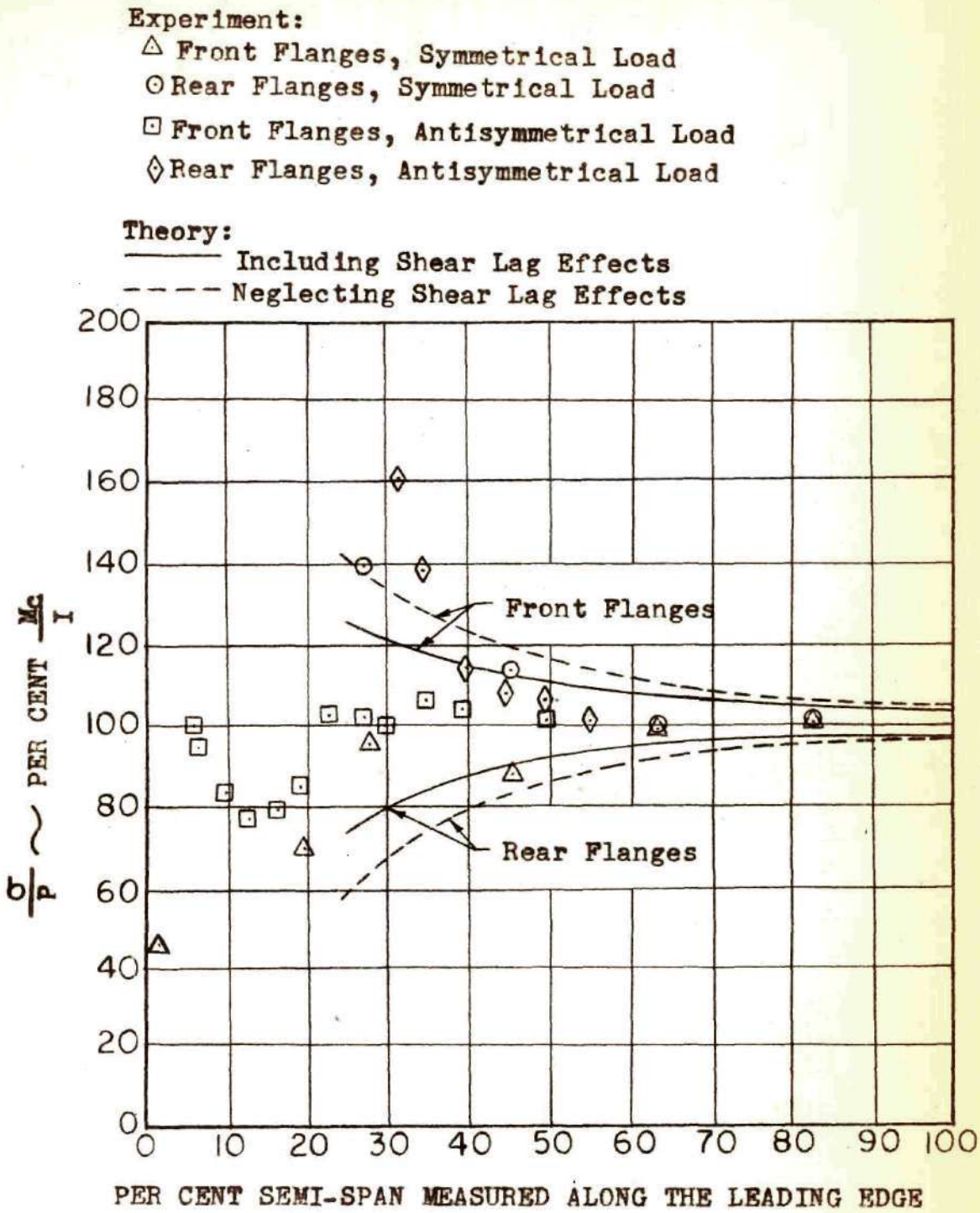

Fig. 9. NORMAL STRESSES IN THE FLANGES OF THE NACA SWEPTBACK BOX BEAM RESULTING FROM UNIT SHEAR LOAD APPLIED AT THE TIP

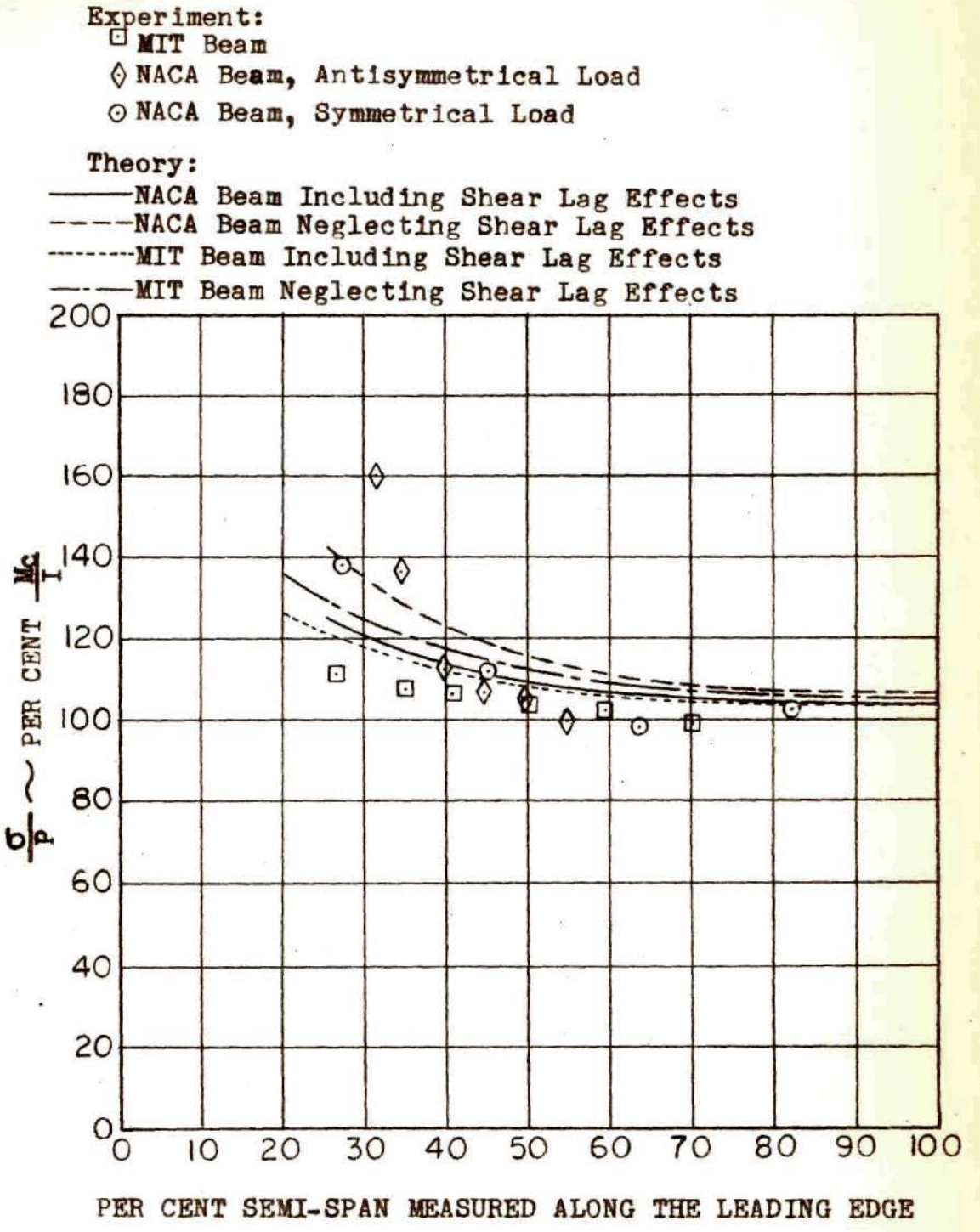

Fig. 10. NORMAL STRESSES IN THE REAR FLANGES OF THE NACA AND MIT SWEPTBACK BOX BEAMS RESULTING FROM UNIT SHEAR LOAD APPLIED AT THE TIP

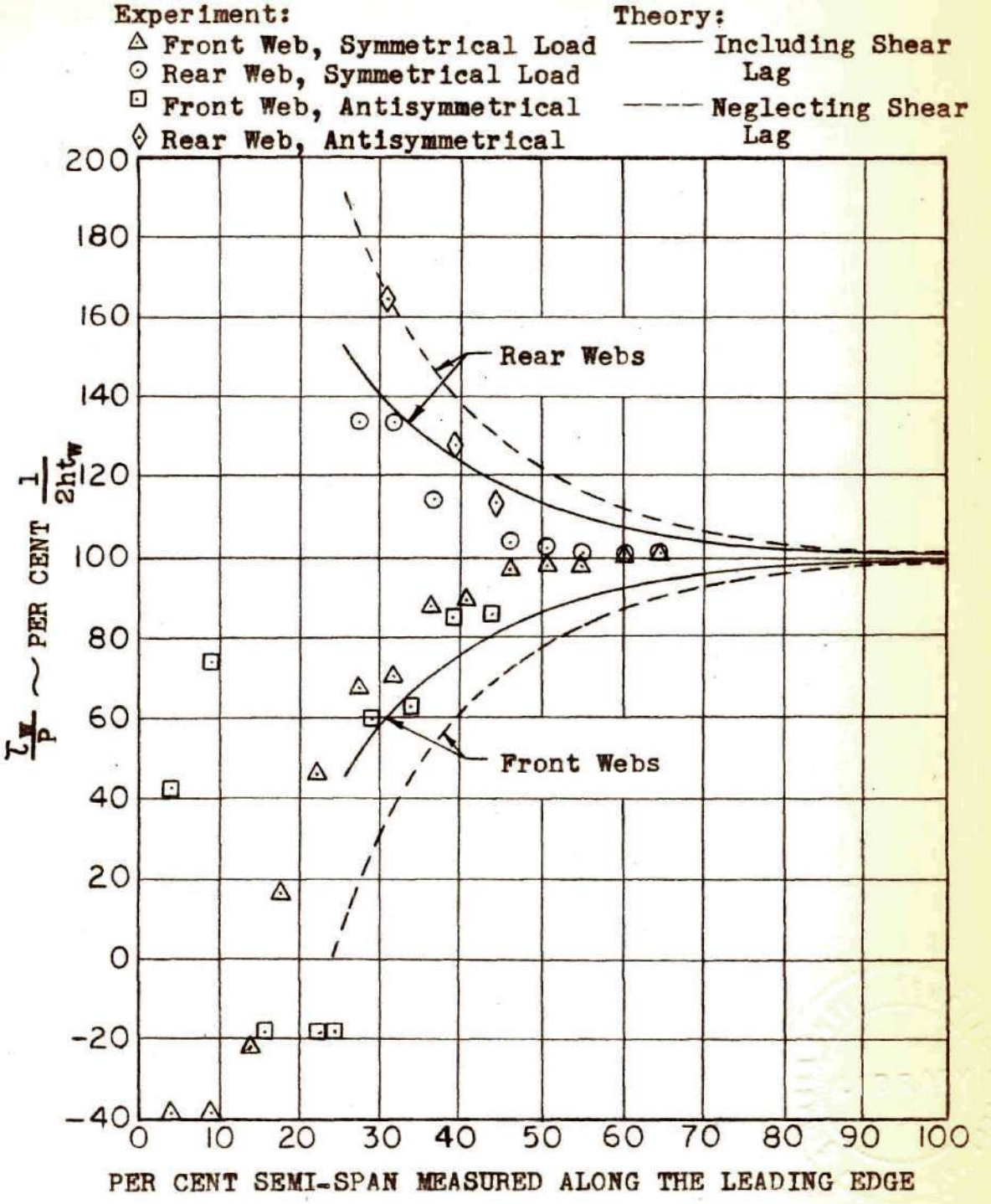

Fig. 11. SHEAR STRESSES IN THE WEBS OF THE NACA SWEPTBACK BOX BEAM RESULTING FROM UNIT SHEAR LOAD APPLIED AT THE TIP

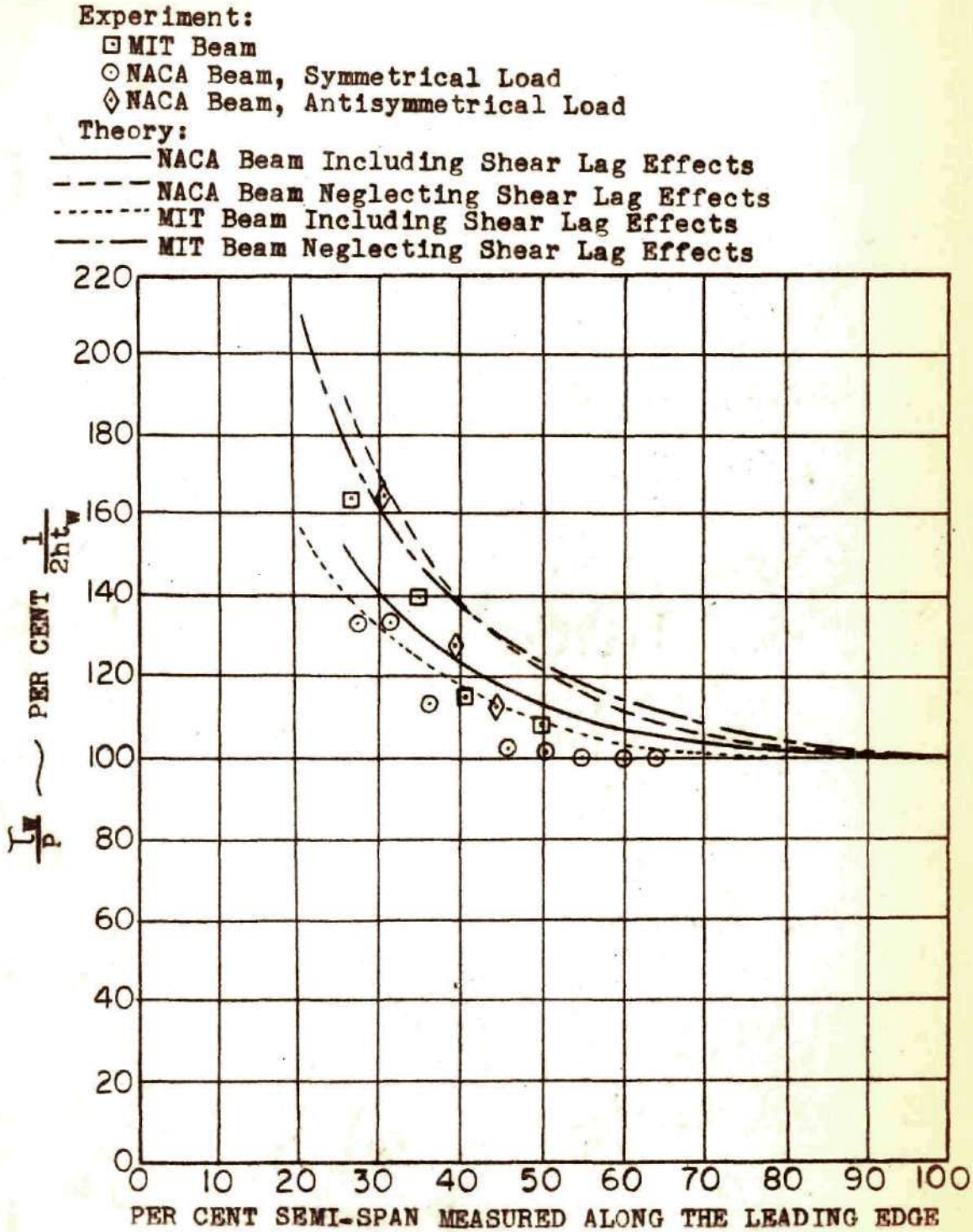

Fig. 12. SHEAR STRESSES IN THE REAR WEBS OF THE NACA AND MIT SWEPTBACK BOX BEAMS RESULTING FROM UNIT SHEAR LOAD APPLIED AT THE TIPS

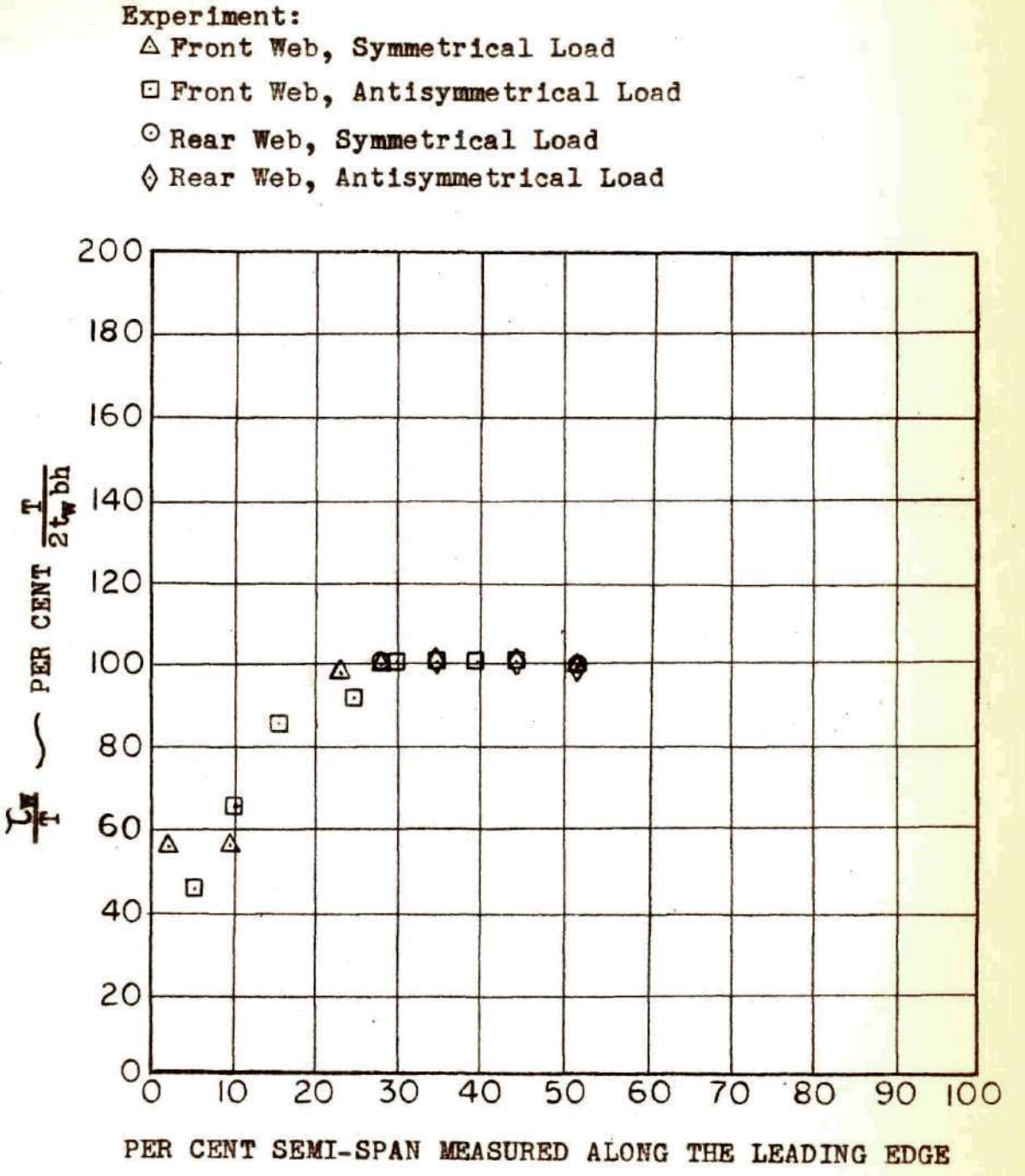

Fig. 13. SHEAR STRESSES IN THE WEBS OF THE NACA SWEPTBACK BOX BEAM RESULTING FROM UNIT TORQUE LOAD APPLIED AT THE TIP

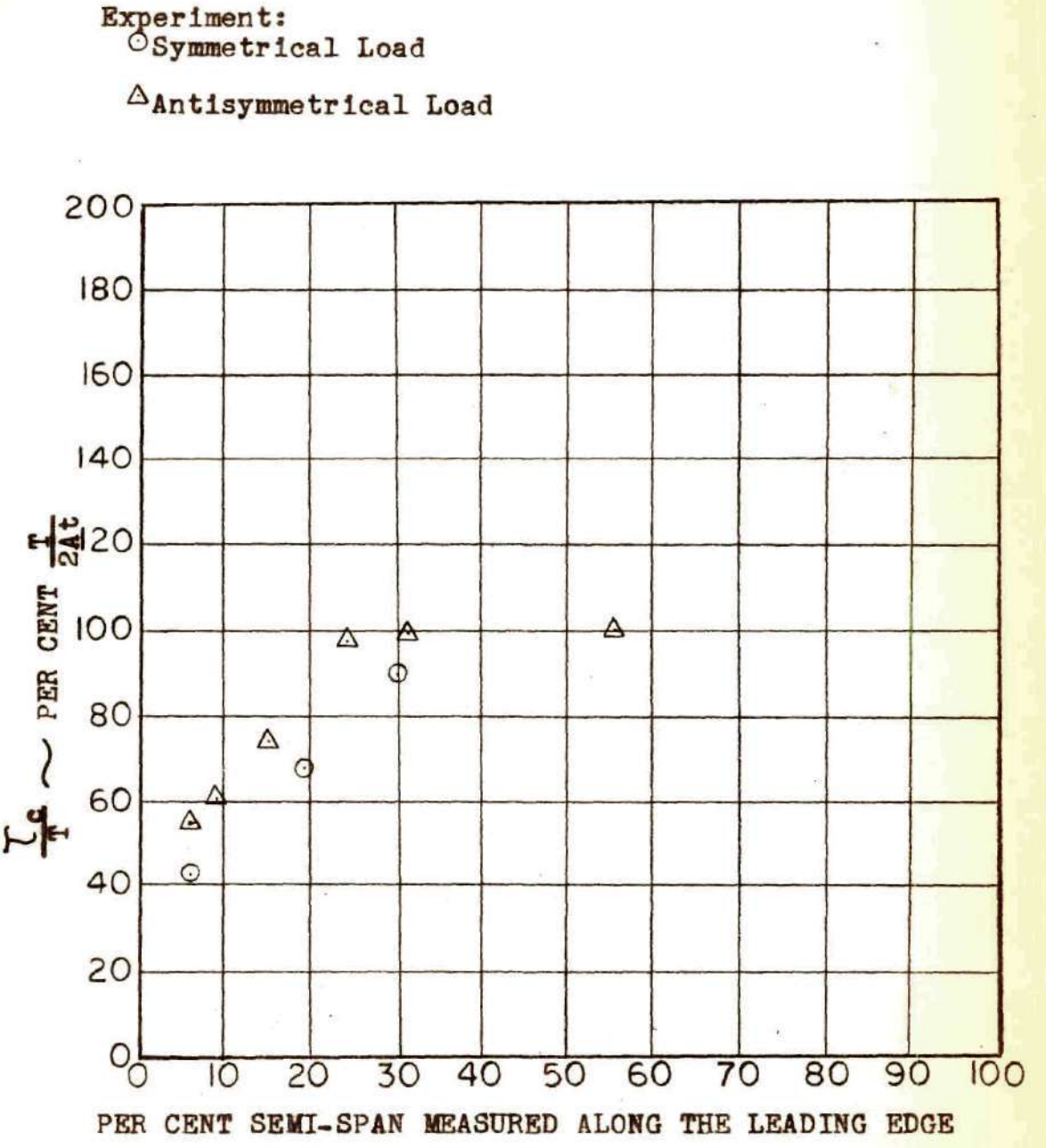

Fig. 14. SHEAR STRESSES IN THE COVERS OF THE NACA SWEPTBACK BOX BEAM RESULTING FROM UNIT TORQUE LOAD APPLIED AT THE TIP